JACS
JOURNAL OF THE AMERICAN CHEMICAL SOCIETY

Communication

pubs.acs.org/JACS

DNA-Catalyzed Hydrolysis of Esters and Aromatic Amides

Benjamin M. Brandsen, Anthony R. Hesser, Marissa A. Castner, Madhavaiah Chandra, and Scott K. Silverman*

Department of Chemistry, University of Illinois at Urbana−Champaign, 600 South Mathews Avenue, Urbana, Illinois 61801, United States

Supporting Information

ABSTRACT: We previously reported that DNA catalysts (deoxyribozymes) can hydrolyze DNA phosphodiester linkages, but DNA-catalyzed amide bond hydrolysis has been elusive. Here we used in vitro selection to identify DNA catalysts that hydrolyze ester linkages as well as DNA catalysts that hydrolyze aromatic amides, for which the leaving group is an aniline moiety. The aromatic amide-hydrolyzing deoxyribozymes were examined using linear free energy relationship analysis. The hydrolysis reaction is unaffected by substituents on the aromatic ring ($\rho \approx 0$), suggesting general acid-catalyzed elimination as the likely rate-determining step of the addition−elimination hydrolysis mechanism. These findings establish that DNA has the catalytic ability to achieve hydrolysis of esters and aromatic amides as carbonyl-based substrates, and they suggest a mechanism-based approach to achieve DNA-catalyzed aliphatic amide hydrolysis.

Deoxyribozymes have been shown to catalyze numerous chemical reactions, many of which involve cleavage or ligation of substrates at phosphodiester linkages.[1] Most of the earliest deoxyribozymes were identified to catalyze RNA cleavage by transesterification, in a reaction analogous to that catalyzed by ribonuclease protein enzymes. Previously, we showed that DNA can catalyze DNA phosphodiester hydrolysis,[2] which is a very challenging reaction because the uncatalyzed half-life (i.e., the $t_{1/2}$ at near-neutral pH and in the absence of divalent metal ion cofactors at 25 °C) is ∼30 million years.[3] Sequence-specific hydrolysis by DNA catalysts identified using in vitro selection[4] in the presence of Zn^{2+} and Mn^{2+} cofactors was shown to proceed with a half-life on the order of 15 min, corresponding to 10^{12} rate enhancement.[2] Subsequently, we showed that Zn^{2+} alone can be the cofactor, with a half-life on the order of 0.5 min and nearly 10^{14} rate enhancement.[5] Although amide (peptide) bond hydrolysis has a much shorter uncatalyzed half-life on the order of hundreds of years,[6] our efforts to achieve DNA-catalyzed amide hydrolysis by in vitro selection have to date been fruitless, instead leading to DNA-catalyzed DNA phosphodiester hydrolysis in our initial report[2] and no DNA-catalyzed amide hydrolysis in several unpublished follow-up efforts. Therefore, DNA-catalyzed amide bond hydrolysis is a major unsolved problem, especially considering the practical value of engineered and artificial protease enzymes.[7] Others have sought nucleic acid catalyzed hydrolysis of carbonyl-based substrates. The group I intron ribozyme has modest aminoacyl esterase activity.[8] This ribozyme was also evolved to cleave an amide bond, using a guanosine nucleophile to attack the amide analogue of the natural phosphodiester substrate, but extending this specific finding to broader peptide cleavage is difficult.[9] Hydrolysis of a cholesteryl carbonate derivative was catalyzed by a ribozyme that was identified indirectly by aptamer selection using a transition state analogue,[10] but the strategy was not applied to amide hydrolysis, and the approach has not proven widely applicable.

In the present study, we systematically and directly pursued DNA-catalyzed hydrolysis of two related types of carbonyl-based substrate, esters and amides. Both esters and amides should be cleavable by hydrolytic addition−elimination mechanisms, and the ease of amide hydrolysis should be tunable by changing the nitrogen substituent. Our results reveal robust DNA-catalyzed ester hydrolysis as well as DNA-catalyzed amide hydrolysis when the nitrogen is substituted with an aromatic ring; i.e., the substrate is an aromatic amide, or anilide. Insight into the mechanism of DNA-catalyzed aromatic amide hydrolysis was obtained from linear free energy relationship analysis. The findings directly demonstrate the feasibility of DNA-catalyzed hydrolysis of carbonyl-based substrates, including for the first time an (aromatic) amide. Our results also suggest mechanism-based approaches to overcome the continuing challenge of DNA-catalyzed hydrolysis of a simple aliphatic amide bond.

DNA-catalyzed hydrolysis of phosphodiester bonds emerged in our previous report despite the availability of several amide bonds in the selection substrate,[2] although many such deoxyribozymes from that and later studies function well with all-DNA substrates.[5c] Therefore, here we applied a stringent selection pressure to allow the survival of DNA sequences only if they catalyze ester or amide hydrolysis but not phosphodiester cleavage (Figure 1). A 40-nucleotide random region (N_{40}) was provided with a covalently attached substrate that presented either an ester or an amide linkage embedded between two DNA oligonucleotide segments, with Watson−Crick base pairs holding the substrate in place. The population of random DNA sequences (each with attached substrate) was incubated under conditions anticipated to be conducive to ester or amide hydrolysis. DNA-catalyzed cleavage of the ester or amide linkage revealed a free carboxylic acid (CO_2H) group, which was captured by splinted reaction with an amino-oligonucleotide and the coupling reagent DMT-MM[11] (Figure

Received: July 26, 2013
Published: October 15, 2013

   dx.doi.org/10.1021/ja4077233 | J. Am. Chem. Soc. 2013, 135, 16014−16017

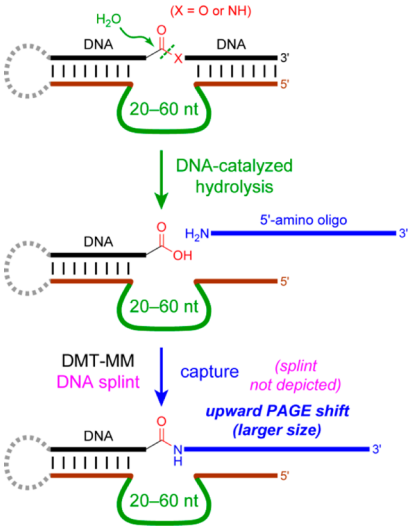

Figure 1. In vitro selection of ester- and amide-hydrolyzing deoxyribozymes. DNA-catalyzed hydrolysis is followed by capture of the revealed carboxylic acid using an amino-oligonucleotide, which results in an upward PAGE shift for the active DNA sequences. See Figure S1 for details. The dashed loop on the left enables the selection process but is dispensable for catalysis.

1; see also Figure S1). Control experiments verified that phosphodiester hydrolysis near the ester or amide linkage did not result in subsequent DMT-MM-activated capture. The amino-oligonucleotide induced a substantial increase in length of the captured deoxyribozyme product, which was readily separated by PAGE and amplified by PCR to enter the next selection round.

Using the strategy of Figure 1, three hydrolysis substrates were subjected to in vitro selection, each under two incubation conditions. The three substrates (Figure 2) included either an

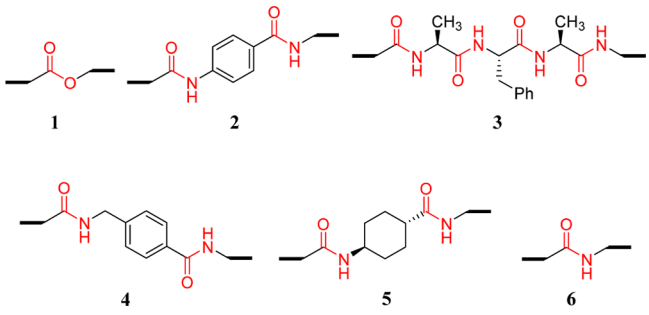

Figure 2. Structures of the ester and amide substrates **1**–**6** used in this study. The horizontal black bars represent DNA oligonucleotide segments. Ester and amide linkages are colored red. See Figure S2 for more detailed structures.

ester linkage (**1**), an aromatic amide (anilide) linkage for which the hydrolytic leaving group is an aniline moiety (**2**), or the Ala-Phe-Ala tripeptide (**3**). The tripeptide substrate **3** was evaluated because of the possibility that simply providing an aromatic ring near the intended reaction site would improve the ability of DNA to interact with the substrate, as has been observed for the "flexizyme" aminoacylation ribozymes.[12] Substrate **2** also includes an aromatic ring, but in addition, the aromatic nitrogen substituent changes the electronic structure of the amide linkage (particularly the nitrogen basicity) and, via ring substitution, provides a derivatization site for mechanistic studies. During the key selection step of each round, the incubation conditions were defined either as (*A*) 70 mM HEPES, pH 7.5, 1 mM $ZnCl_2$, 20 mM $MnCl_2$, 40 mM $MgCl_2$, and 150 mM NaCl at 37 °C or as (*B*) 50 mM CHES, pH 9.0, 40 mM $MgCl_2$, and 150 mM NaCl at 37 °C. Each of the Zn^{2+}, Mn^{2+}, and Mg^{2+} ions have been effective deoxyribozyme cofactors in many prior selection experiments, but Zn^{2+} and Mn^{2+} cannot be used above pH 7.5 due to precipitation and oxidation, respectively.

Both of the selections for ester hydrolysis using substrate **1** led to strong catalytic activity (see all selection progressions in Figure S3), despite a nontrivial background ester cleavage rate under both incubation conditions (4% background hydrolysis in 14 h under conditions *A*, and 4% background hydrolysis in 1 h under conditions *B*). Under conditions *A*, after 10 rounds in which each selection step was performed for 14 h, the hydrolysis yield of the DNA pool reached 49%. Under conditions *B*, after 13 rounds with each selection step performed for 1 h, the pool yield was 38%. Both pools were cloned, and individual deoxyribozymes were characterized as described below. Separately, of the two selections for aromatic amide hydrolysis with substrate **2**, only the effort using conditions *A* led to activity. After 8 rounds with each selection step performed for 14 h, the pool yield was 36%, and individual deoxyribozymes were cloned and characterized. In contrast, the experiment using conditions *B* led to no detectable activity (<0.5%) after 17 rounds. Finally, neither of the two selections with the Ala-Phe-Ala substrate **3** led to detectable activity (<0.5%) after 17 rounds. Sequences of all deoxyribozymes are provided in Figure S4.

Individual deoxyribozymes were characterized for each of the three selection experiments that led to substantial catalytic activity, with product identities established by mass spectrometry (Figure S5). Eleven and three unique ester-hydrolyzing deoxyribozymes that cleave substrate **1** were identified from the selections under respective conditions *A* (pH 7.5 with Zn^{2+}/Mn^{2+}/Mg^{2+}) and *B* (pH 9.0 with Mg^{2+}).[13] The 14 sequences are essentially unrelated to one another (Figure S4A). The single-turnover rate constants were as high as k_{obs} = 0.54 h^{-1} (10ZA8 under conditions *A*) and 3.1 h^{-1} (13ZB38 under conditions *B*), with hydrolysis yields up to 90% (Figures 3 and S6). These k_{obs} values correspond to rate enhancements of up to 240, computed relative to the uncatalyzed ester hydrolysis rate constants under the corresponding incubation conditions. The eleven deoxyribozymes for conditions *A* all responded similarly to changes in pH by showing maximal yield at pH 7.5, although in some cases activity was maintained at pH 7.2 or 7.8 (Figure S7A). The three deoxyribozymes for conditions *B* were all faster at higher pH over the range 7.5 through 10 (Figure S7B). The metal ion dependence of each deoxyribozyme was also examined (Figure S8). Of the eleven deoxyribozymes for conditions *A*, all required Zn^{2+} for optimal activity; seven additionally required Mn^{2+}, and two additionally required both Mn^{2+} and Mg^{2+} for optimal activity. Each of the three deoxyribozymes for conditions *B* required Mg^{2+} (noting that conditions *B* omit both Zn^{2+} and Mn^{2+}).

Five anilide-hydrolyzing deoxyribozymes that cleave substrate **2** emerged from the selections under conditions *A* (pH 7.5 with Zn^{2+}/Mn^{2+}/Mg^{2+}; 36% pool yield at round 8). Sequence alignment (Figure S4B) shows two regions of substantial conservation flanking a central variable region. The two DNA catalysts with the highest yields, 8ZC9 and 8ZC30, had single-turnover k_{obs} values of 0.13 ± 0.01 h^{-1} (*n* =

dx.doi.org/10.1021/ja4077233 | J. Am. Chem. Soc. 2013, 135, 16014–16017

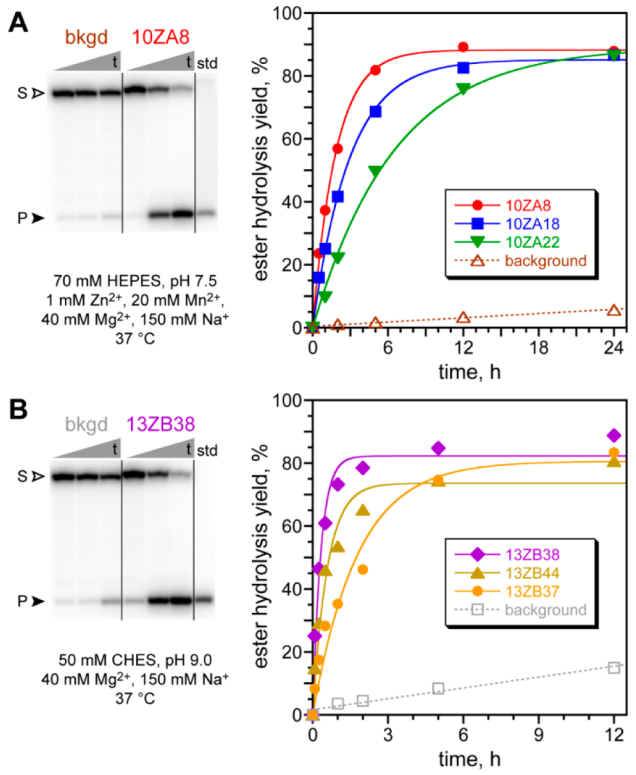

Figure 3. PAGE images and kinetic plots for ester-hydrolyzing deoxyribozymes. S = substrate **1**; P = cleavage product. PAGE images show time points at t = 30 s, 30 min, and 12 h for one representative deoxyribozyme from each set. (A) Deoxyribozymes identified from the selection under conditions *A*. k_{obs} values: 0.54, 0.34, 0.15 h^{-1}; k_{bkgd} 0.0024 h^{-1}. See Figure S6 for data for the other eight 10ZA deoxyribozymes. (B) Deoxyribozymes identified from the selection under conditions *B*. k_{obs} values: 3.1, 1.7, 0.56 h^{-1}; k_{bkgd} 0.013 h^{-1}. See Figures S7 and S8 for detailed pH and metal ion requirements.

4) and 0.21 ± 0.03 h^{-1} (n = 5), respectively, and hydrolysis yields up to 80% (Figure 4). These k_{obs} values correspond to rate enhancements of >3600 and >5000 (background hydrolysis undetected, <0.4% in 96 h). Each deoxyribozyme had maximal activity at pH 7.5, with generally little activity at pH 7.2 or 7.8 (Figure S9). All five deoxyribozymes required both Zn^{2+} and Mn^{2+}; in two cases including 8ZC9, Mg^{2+} was additionally required for optimal activity (Figure S10). When

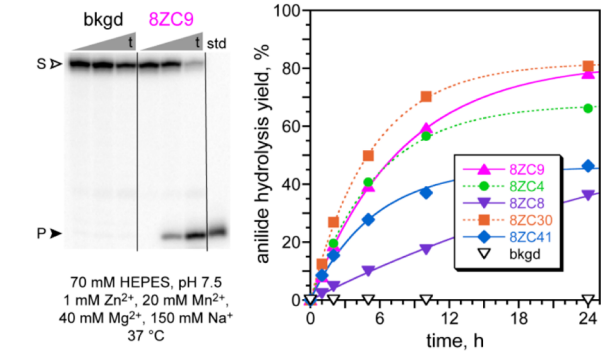

Figure 4. Activities of aromatic amide-hydrolyzing deoxyribozymes identified from the selection under conditions *A*. k_{obs} values (top to bottom in legend): 0.13, 0.18, 0.028, 0.19, 0.18 h^{-1}; k_{bkgd} <0.00004 h^{-1}. Only the anilide bond of substrate **2** is hydrolyzed (Figure S5). See Figures S9 and S10 for detailed pH and metal ion requirements.

8ZC9 was partially randomized (25% per nucleotide) and reselected for hydrolysis of **2**, after 6 rounds (33% pool yield) a set of 13 related sequences was identified, showing the same conservation pattern as for the parent 8ZC deoxyribozymes (Figure S4B). These reselected DNA catalysts had k_{obs} values up to 3-fold higher than that of 8ZC9 (data not shown).

We recently showed that, for other DNA-catalyzed reactions, the outcome of in vitro selection depends critically on the length of the random region; e.g., larger random regions explore more complex structures but are sampled less thoroughly.[14] Here we evaluated N_{20}, N_{30}, N_{50}, and N_{60} regions with anilide substrate **2** and conditions *A* (pH 7.5 with Zn^{2+}/Mn^{2+}/Mg^{2+}), rather than N_{40} as used to identify the 8ZC deoxyribozymes. The N_{50} and N_{60} selections gave no activity through round 11 and were discontinued. In contrast, the N_{20} and N_{30} selections led to 49% cleavage at round 9 and 33% cleavage at round 8, respectively. The new N_{20} deoxyribozymes—which among themselves shared a largely conserved sequence—had no conservation when compared to the N_{40}-derived 8ZC deoxyribozymes (Figure S4C); k_{obs} values were similar to those for 8ZC9 (data not shown), as was the yield optimum at pH 7.5 (Figure S11A). The new N_{20} deoxyribozymes functioned well with Zn^{2+} as the sole divalent metal ion, without requiring either Mn^{2+} or Mg^{2+}. In parallel, the eight new N_{30} deoxyribozymes retained both conserved sequence elements of the N_{40}-derived 8ZC deoxyribozymes (Figure S4C). The N_{30} k_{obs} values were similar to those of the N_{40} deoxyribozymes (data not shown), and the yield was optimal at pH 7.5 (Figure S11B). The N_{30} deoxyribozymes also shared the requirement for Zn^{2+} and Mn^{2+} (but not Mg^{2+}) with most of their N_{40} counterparts. In summary, of the N_{20}–N_{60} experiments, only the smaller N_{20}, N_{30}, and N_{40} random regions led to catalytic activity, and the sequences and metal ion dependences of the N_{20} DNA catalysts were distinct from those of the N_{30} and N_{40} deoxyribozymes.

Each of the 8ZC deoxyribozymes was evaluated with substrate **4** (Figure 2) that retains the aromatic ring of **2** but includes a methylene group between the aromatic ring and the former anilide nitrogen atom (i.e., the leaving group is benzylamine rather than aniline). Each 8ZC deoxyribozyme was also tested with substrate **5** that replaces the benzene ring of **2** with cyclohexane. In all cases, no activity was observed (<0.5%; data not shown). Unsurprisingly given these results, aliphatic amide **6**—which is structurally analogous to ester **1** but has an aliphatic amide moiety in place of the ester—is also not cleaved by these DNA catalysts. Substrate **2** offers two distinct amide bonds for cleavage: an aromatic amide for which the leaving group is aniline, and a benzamide for which the leaving group is a primary aliphatic amine. The only observed hydrolysis reaction for **2** was cleavage of its aromatic amide (Figure S5). Alongside the lack of catalytic activity from the selection using the Ala-Phe-Ala substrate **3**, these results indicate that the mere presence of an aromatic ring in the substrate is insufficient to promote DNA-catalyzed hydrolysis. Instead, the identity of the leaving group as an aniline rather than an aliphatic amide enabled the reaction.

No DNA catalysts emerged from direct selections using **6** with N_{20}–N_{60} random regions (data not shown). We also made several attempts to evolve ester- and anilide-hydrolyzing deoxyribozymes into DNA catalysts for hydrolysis of aliphatic amide **6**, considering that both ester and amide hydrolysis should proceed through addition–elimination mechanisms. Toward this goal, numerous ester-hydrolyzing 10ZA deoxy-

dx.doi.org/10.1021/ja4077233 | J. Am. Chem. Soc. 2013, 135, 16014–16017

ribozymes and anilide-hydrolyzing 8ZC deoxyribozymes were partially randomized (25% per nucleotide) and reselected for cleavage of **6**. In all cases, however, no activity was observed (data not shown).

To investigate the mechanistic basis for the observed DNA-catalyzed hydrolysis of aromatic amide **2**, linear free energy relationships (LFERs) were obtained. Substituents were placed individually onto the aromatic ring of **2** in the position *ortho* to the anilide nitrogen atom, noting that the *para* position is already occupied by the benzamide carbonyl group. The hydrolysis rate constants k_{obs} for all five 8ZC deoxyribozymes (N_{40}) were determined for several electron-donating substituents [$\sigma_p < 0$: $(CH_3)_2NH$, CH_3O and CH_3] as well as electron-withdrawing substituents [$\sigma_p > 0$: Cl and CF_3]. Each plot of $\log(k_X/k_H)$ versus σ_p was linear with slope $\rho \approx 0$ (Figures 5 and S12). These LFER data are consistent with an

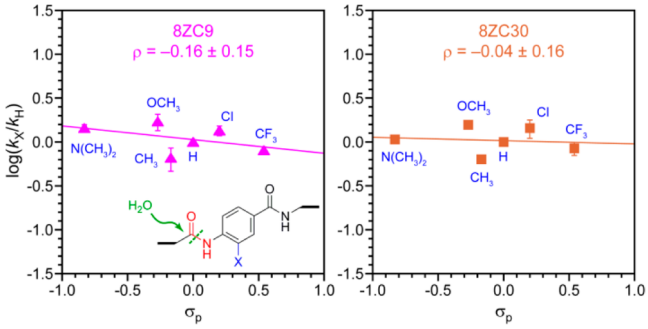

Figure 5. LFER data for the 8ZC9 and 8ZC30 deoxyribozymes. See Supporting Information for details.

addition−elimination mechanistic model in which aromatic amide hydrolysis proceeds with rate-determining general acid-catalyzed elimination involving nitrogen protonation (see Figure S13 for a full explanation of this conclusion). We also note that other mechanistic explanations are possible, e.g., involving a rate-determining conformational change. When the phenol analogue of **2** was tested with the five 8ZC deoxyribozymes, substantial activity (k_{obs} 5- to 33-fold above k_{bkgd} = 0.4 h^{-1}) was observed for all but 8ZC4 (Figure S14). This finding indicates that at least two distinguishable modes of interaction are possible between an anilide-hydrolyzing DNA catalyst and its substrate.

In summary, we have demonstrated that DNA can catalyze hydrolysis of esters and aromatic amides (anilides). Linear free energy relationship analysis of the anilide-hydrolyzing deoxyribozymes suggests that the rate-determining mechanistic step involves concomitant nitrogen protonation and C−N bond cleavage. What explains the absence of deoxyribozymes for hydrolysis of aliphatic amides such as substrate **6**? A reasonable hypothesis is that the decreased electrophilicity of the carbonyl carbon of **6** relative to **2** shifts the rate-determining step for potential deoxyribozymes to carbonyl addition rather than elimination. If correct, then identifying these deoxyribozymes requires accelerating the addition step, e.g., by use of a stronger nucleophile such as an amine rather than water. Our current efforts are evaluating this hypothesis. In the longer term, deoxyribozymes for amide cleavage will be developed for free peptide and protein substrates, as we have recently established for phosphatase activity.[15]

■ ASSOCIATED CONTENT

Supporting Information

Experimental details and additional data. This material is available free of charge via the Internet at http://pubs.acs.org.

■ AUTHOR INFORMATION

Corresponding Author

scott@scs.illinois.edu

Notes

The authors declare no competing financial interest.

■ ACKNOWLEDGMENTS

This research was supported by grants to S.K.S. from the National Institutes of Health (R01GM065966), the Defense Threat Reduction Agency (HDTRA1-09-1-0011), and the National Science Foundation (CHE0842534). B.M.B. was partially supported by NIH T32 GM070421.

■ REFERENCES

(1) (a) Silverman, S. K. *Nucleic Acids Res.* **2005**, *33*, 6151. (b) Schlosser, K.; Li, Y. *Chem. Biol.* **2009**, *16*, 311. (c) Silverman, S. K. *Angew. Chem., Int. Ed.* **2010**, *49*, 7180.

(2) Chandra, M.; Sachdeva, A.; Silverman, S. K. *Nat. Chem. Biol.* **2009**, *5*, 718.

(3) Schroeder, G. K.; Lad, C.; Wyman, P.; Williams, N. H.; Wolfenden, R. *Proc. Natl. Acad. Sci. U.S.A.* **2006**, *103*, 4052.

(4) (a) Joyce, G. F. *Annu. Rev. Biochem.* **2004**, *73*, 791. (b) Joyce, G. F. *Angew. Chem., Int. Ed.* **2007**, *46*, 6420. (c) Silverman, S. K. *Chem. Commun.* **2008**, 3467.

(5) (a) Xiao, Y.; Chandra, M.; Silverman, S. K. *Biochemistry* **2010**, *49*, 9630. (b) Xiao, Y.; Allen, E. C.; Silverman, S. K. *Chem. Commun.* **2011**, *47*, 1749. (c) Xiao, Y.; Wehrmann, R. J.; Ibrahim, N. A.; Silverman, S. K. *Nucleic Acids Res.* **2012**, *40*, 1778.

(6) Radzicka, A.; Wolfenden, R. *J. Am. Chem. Soc.* **1996**, *118*, 6105.

(7) (a) Varadarajan, N.; Rodriguez, S.; Hwang, B. Y.; Georgiou, G.; Iverson, B. L. *Nat. Chem. Biol.* **2008**, *4*, 290. (b) Yoo, T. H.; Pogson, M.; Iverson, B. L.; Georgiou, G. *ChemBioChem* **2012**, *13*, 649. (c) Ameta, S.; Jäschke, A. *Chem. Sci.* **2013**, *4*, 957.

(8) Piccirilli, J. A.; McConnell, T. S.; Zaug, A. J.; Noller, H. F.; Cech, T. R. *Science* **1992**, *256*, 1420.

(9) Dai, X.; De Mesmaeker, A.; Joyce, G. F. *Science* **1995**, *267*, 237; Correction: *Science* **1996**, *272*, 18.

(10) Chun, S.-M.; Jeong, S.; Kim, J.-M.; Chong, B.-O.; Park, Y.-K.; Park, K.; Yu, J. *J. Am. Chem. Soc.* **1999**, *121*, 10844.

(11) Kunishima, M.; Kawachi, C.; Hioki, K.; Terao, K.; Tani, S. *Tetrahedron* **2001**, *57*, 1551.

(12) Morimoto, J.; Hayashi, Y.; Iwasaki, K.; Suga, H. *Acc. Chem. Res.* **2011**, *44*, 1359.

(13) Each deoxyribozyme was named as (for example) 10ZA8, where 10 is the round number, ZA is the systematic alphabetical designation for the particular selection, and 8 is the clone number.

(14) Velez, T. E.; Singh, J.; Xiao, Y.; Allen, E. C.; Wong, O.; Chandra, M.; Kwon, S. C.; Silverman, S. K. *ACS Comb. Sci.* **2012**, *14*, 680.

(15) Chandrasekar, J.; Silverman, S. K. *Proc. Natl. Acad. Sci. U.S.A.* **2013**, *110*, 5315.